MDPI

Article

The Production Analysis and Exploitation Scheme Design of a Special Offshore Heavy Oil Reservoir—First Offshore Artificial Island with Thermal Recovery

Guodong Cui [1,2,3,*], Zheng Niu [1] , Zhe Hu [1], Xueshi Feng [1] and Zehao Chen [1]

1   National Center for International Research on Deep Earth Drilling and Resource Development, Faculty of Engineering, China University of Geosciences, Wuhan 430074, China
2   School of Sustainable Energy, China University of Geosciences, Wuhan 430074, China
3   Shenzhen Research Institute, China University of Geosciences, Shenzhen 518000, China
*   Correspondence: cuiguodong@cug.edu.cn

Abstract: More and more offshore heavy oil resources are discovered and exploited as the focus of the oil and gas industry shifts from land to sea. However, unlike onshore heavy oil reservoirs, offshore heavy oil reservoirs not only have active edge and bottom water but also have different exploitation methods. In this paper, a typical special heavy oil reservoir in China was analyzed in detail, based on geology–reservoir–engineering integration technology. Firstly, it is identified as a self-sealing bottom water heavy oil reservoir by analyzing its geological characteristics and hydrocarbon accumulation mechanism. Secondly, the water cut is initially controlled by oil viscosity, but subsequently, by reservoir thickness through the analysis of oil and water production data. Thirdly, the bottom oil–water contact of the reservoir was re-corrected to build an accurate 3D geological model, based on the production history matching of a single well and the whole reservoir. Lastly, a scheme of thermal production coupled with cold production was proposed to exploit this special reservoir, and the parameters of steam, N_2, and CO_2 injection and production were optimized to predict oil production. This work can provide a valuable development model for the efficient exploitation of similar offshore special heavy oil reservoirs.

Keywords: offshore; heavy oil reservoir; steam huff and puff; water invasion; exploitation scheme

1. Introduction

1.1. Offshore Heavy Oil

Heavy oil resources are very rich in the world, with geological reserves of about 815 billion tons, accounting for 70% of the remaining global oil reserves, mainly distributed in Canada, Venezuela, Russia, the United States, and China [1]. It is an alternative to conventional oil and an important raw material for processing aerospace fuel, high-grade oil, and so on. Therefore, sustainable and efficient exploitation of heavy oil is of great practical significance for maintaining national energy security [2].

The reserves of heavy oil resources explored in China are 43.5×10^8 t, accounting for more than 20% of the total oil resources, mainly distributed in Bohai Bay, Songliao Basin, Tarim Basin, Turpan-Hami Basin, and the North China Plain [3]. In recent years, through theoretical innovation and technological breakthroughs, the annual production of heavy oil has stabilized at $1500\sim1600 \times 10^4$ t, accounting for about 8% of China's annual oil production, and has become an important part of crude oil production in China.

The choice of exploitation method for heavy oil is closely related to its burial depth. For shallow heavy oil reservoirs (depth < 75 m), open-pit mining is generally used for exploitation. For deep buried reservoirs (depth > 75 m), drilling combined with thermal and cold recovery technologies are generally used for in situ exploitation; especially, thermal recovery technology is mainly adopted [4–6]. Among them, steam huff and puff is the most

commonly used method in current thermal recovery technologies, which consists of three stages: steam intake, steam soak, and steam ejection in the same well [7]. Physically, the injected steam can heat the heavy oil and, hence, decrease the oil viscosity dramatically, so the mobility ratio of oil to water increases and more oil is extracted. Up to now, steam huff and puff has been widely applied in Liaohe [8], Xinjiang, and other onshore heavy oilfields in China [9,10].

As the focus of the oil and gas industry in China shifts from land to sea, more and more offshore heavy oil resources have been found and exploited. Among them, the Bohai Sea area has the most abundant heavy oil resources with geological reserves of 700 million tons, accounting for 95% of the country's heavy oil reserves. It has become a key area for the exploitation of offshore heavy oil in China [11,12]. However, unlike onshore heavy oil, offshore heavy oil always exists with high fluid pressure, active edge, and bottom water, which increases the difficulty of exploitation [13]. Notably, the overlying seawater increases the well length and well heat loss [14], so the input cost is high [15].

What is more interesting is that more and more special heavy oil reservoirs have been encountered in the development of heavy oil in the Bohai Sea area, China [16,17]. The physical properties of the heavy oil in the reservoir are different from those of common heavy oil onshore. For example, the oil distribution is not controlled by the geological structure or lithology, and the oil viscosity is not uniformly distributed in the region. The thermal recovery method usually applied in onshore heavy oil fields fails to achieve the desired goal of increasing oil production. For example, steam huff and puff can reduce the water cut in some areas, but the water cut increases after the steam injection in other areas. More particularly, conventional cold recovery technology can also achieve stable oil production for a period of time in some areas. These are different from conventional heavy oil production after steam huff and puff, resulting in low exploitation efficiency.

1.2. Existing Problems

(1) The target heavy oil reservoir is a special type of reservoir

The horizontal oil–water contact of the reservoir is irregular and its distribution is not controlled by the geological structure. The vertical oil–water contact is discontinuous, and its distribution is not controlled by gravity. The oil viscosity presents a complex spatial distribution, with the overall performance of high oil viscosity at the oil–water boundary but low oil viscosity in the central region. These unique characteristics make it difficult to define or classify the reservoir using the conventional hydrocarbon accumulation mechanism. Therefore, it is necessary to evaluate the oil accumulation distribution of this type of reservoir in combination with geological data and oil production analysis, to guide the optimization of current oil production and the formulation of subsequent development plans.

(2) Production of oil and water differs from conventional heavy oil

Different from conventional heavy oil reservoirs, steam huff and puff in some areas of the study reservoir can improve the oil recovery but is not effective in other areas. Instead, conventional cold production can be adopted to enhance oil recovery and stabilize oil production over a period of time. It can be seen that the conventional exploitation methods and steam huff and puff measures in onshore heavy oil reservoirs cannot be copied and applied to this type of reservoir. Especially, during the process of studying the oil and water production, it is found that the relation between water cut and liquid production differs from that of conventional bottom water heavy oil reservoirs, and the increase in water cut is often earlier than the liquid production. Considering the influence of the oil–water mobility ratio and interface on oil production, it is preliminarily concluded that the distinctive characteristic of oil and water production is related to the oil viscosity distribution. However, whether these anomalies are also related to other factors, such as the bottom oil–water contact, needs to be further analyzed from the geological characteristics and the reservoir engineering.

(3)   Steam huff and puff parameter optimization and reasonable exploitation scheme

In the studied oil reservoir, steam huff and puff can effectively reduce the water cut in most wells, but the water cut increases instead of decreases after steam injection for a considerable number of wells. Therefore, for this special offshore heavy oil reservoir, it is necessary to further optimize the parameters of steam huff and puff and design a reasonable exploitation scheme. As commonly used assisted gases, N_2 and CO_2 can increase oil production by inhibiting bottom water rise by raising pressure [18]. In addition, as a good oil displacement agent [19], CO_2 has a higher solubility and greater viscosity reduction effect than nitrogen. Whether the nitrogen- or CO_2-assisted steam huff and puff can significantly increase the oil production in this reservoir needs to be analyzed. Therefore, it is necessary to design a reasonable exploitation scheme to optimize the subsequent heavy oil production process from the perspective of geology–engineering integration.

1.3. Research Methodology

How to efficiently exploit this special type of offshore heavy oil is not only a new challenge but also a new opportunity for China and even the global offshore oil field. Therefore, a systematic and scientific approach for conducting research, gathering data and information, and investigating problems was prepared. Specifically, in Section 1, we outlined the main research questions and objectives of this paper. In Section 2, the reservoir characteristics, oil density, and oil viscosity distribution of a typical special heavy oil reservoir were collected and analyzed in detail to identify the oil reservoir type, based on the world's first heavy oil field using thermal recovery technology. In Section 3, the oil and water production data were analyzed, and the effect of steam huff and puff on oil recovery was evaluated. In Section 4, a three-dimensional geological model and heavy oil thermal recovery simulation model were established and corrected by performing a history matching of production data. In Section 5, a new exploitation scheme of thermal combined with cold recovery was designed and discussed through the understanding of reservoir type, thermal recovery, and geological model. It is hoped that the research can provide practical development guidance and form an effective exploitation scheme for the efficient development of the offshore heavy oil in the world.

2. Geological Description and Analysis

2.1. Site Location

The world's first offshore heavy oil field using thermal recovery technology, Y oilfield (4 November 2013), is located in the shallow sea area to the north of Bohai Bay, China, as shown in Figure 1. It is 40 km away from Panjin City, Liaoning Province, and 18.5 km away from the coast. There are four artificial islands at sea, one onshore terminal, and submarine pipelines and cables are laid between the artificial islands and between the central artificial islands and the mainland [20]. The exploration of the Y oilfield began in the early 1980s, and it holds an estimated 80 million tons of technically recoverable heavy oil according to the assessment by reference [21]. The target reservoir in the paper, NgI reservoir, is recently exploited in the Y oilfield.

2.2. Geological Structure Characteristic

The Y oilfield is located at the southern end of the Hainan–Yuedong drape structural belt and the hanging wall of the Yuedong and Hainan faults, as shown in Figure 2. It is bounded by the Yuedong and Hainan faults in the west, and adjacent to the Crescent structure and Hainan Depression. It is a Cenozoic continental sedimentary basin located in the Liaohe beach area in the north of Bohai Bay Basin and belongs to the transition area between the Liaohe Depression and Liaodong Bay Depression [22,23]. The Liaohe Beach area consists of nine sub-ordinary positive structural belts and two sub-ordinary negative structural belts, and Y oilfield is located at the southern end of the Liaohe Beach Sea central bulge, which is a natural extension of the Liaohe Depression central bulge to the sea. The geological structure of the target reservoir, NgI reservoir, is relatively gentle from the depth

contour map, and there is only one large fault in the west. By comparing with the oil distribution, it can be seen that the oil accumulation is not consistent with the geological structure, and hence, it is not controlled by the geological structure.
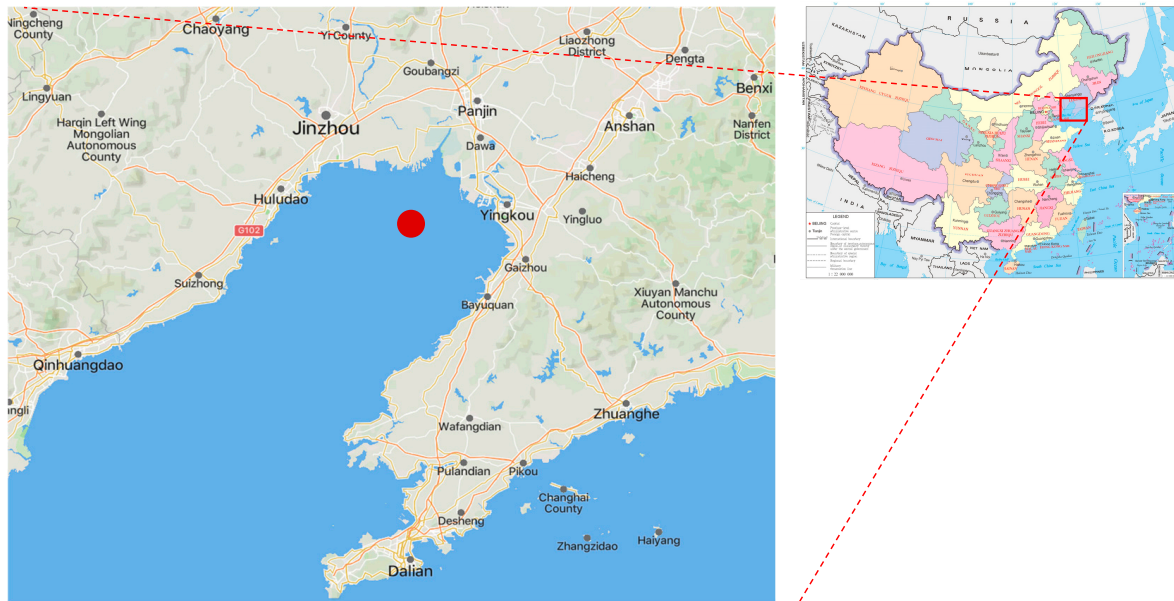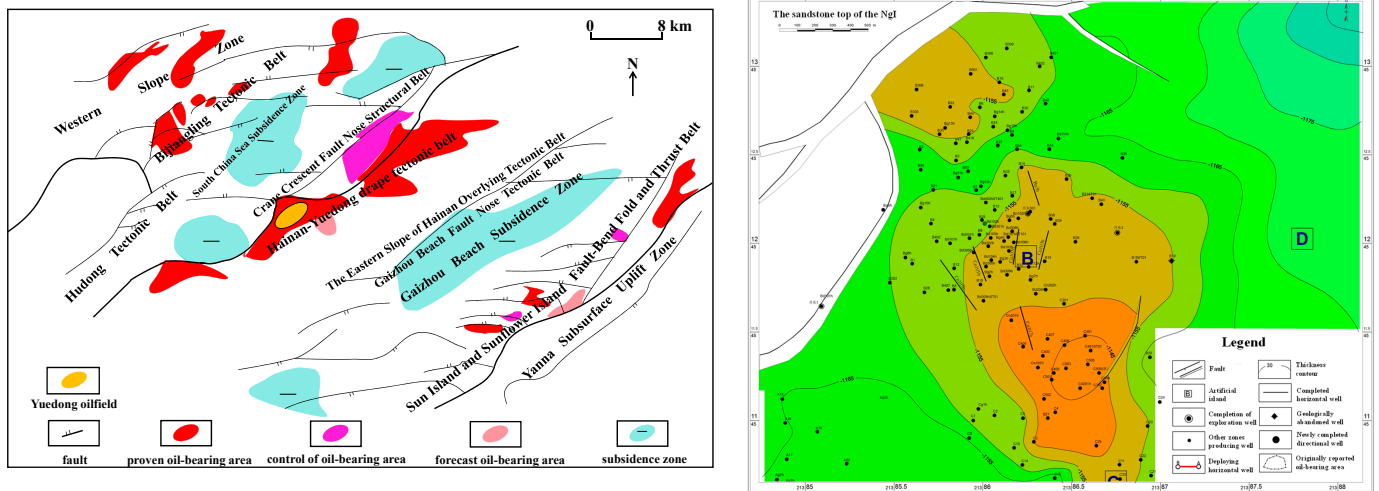

Figure 1. Site location of Y oilfield.

Figure 2. Geological structural distribution and depth contour of the target reservoir top.

2.3. Sedimentary Characteristics

During the sedimentary period of the Neogene Guantao Formation, the lake level of the Bohai Sea fluctuated frequently, and the rate of sediment supply changed accordingly [24]. The study area is located in the eastern part of the delta deposit of Bohai Bay [25–29], and the Guantao Formation sedimentation can be divided into three stages from the bottom to the top: braided river delta deposit, delta-bin shallow lake deposit, and delta deposit. As can be seen from Figure 3, the target oil reservoir belongs to the plain of the braided river delta deposit and consists of channel and alluvial plains. The main body of the target oil reservoir is river sediment, followed by alluvial plain. It can be seen that the overall direction extends from the northeast to the southwest from the analysis of the main river.
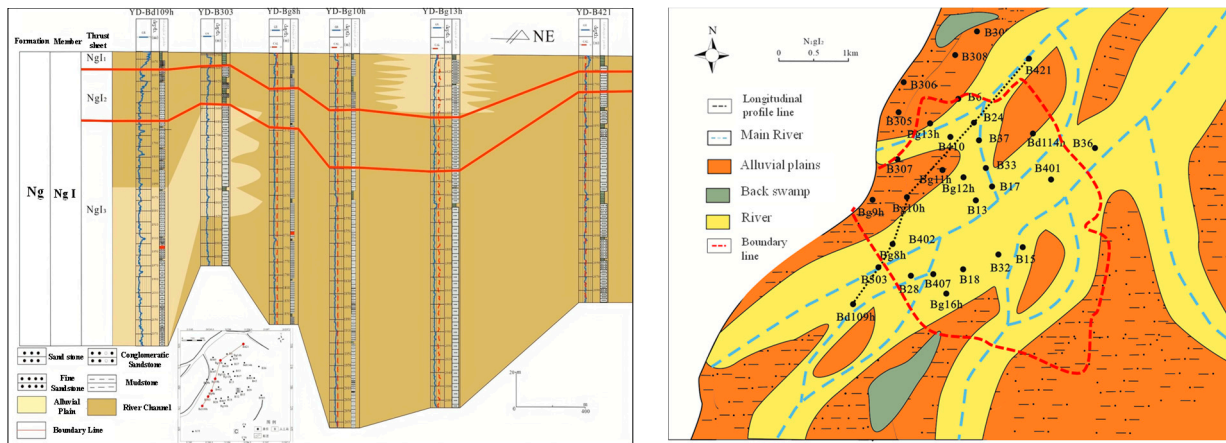
Figure 3. Longitudinal and planar distributions of deposition facies of the target reservoir NgI.

2.4. Formation Characteristic

As shown in Table 1, the strata in the study area are as follows: Archean, Paleozoic, Lower Tertiary Dongying Formation II, Dongying Formation I, and Upper Tertiary Guantao Formation. The Upper Tertiary Guantao Formation is the target oil-bearing layer, and a set of oil-rich sandstone, gravelly sandstone, and sandy conglomerate are developed at its bottom. The vertical physical property of the formation shows positive rhythm, and its thickness ranges from 100 m to 500 m. The thick sandy conglomerate in the bottom has a large storage space, and the top mudstone can serve as a good cap rock. Generally, there are some lithologic variations in the target formation, but the overall change is minor, and the oil distribution is not controlled by the reservoir lithology.

Table 1. The strata in the study area.

Erathem	System	Series	Formation	Thickness, m	
Cenozoic	Neogene	Miocene	Guantao	100~500	Sand conglomerate and sandstone, and there is a set of oil-rich sandstone, pebbled sandstone, and sand conglomerate assemblages at the bottom
	paleogene	Oligocene	Dongying	150~190	Gray-white medium coarse sandstone, medium sandstone, fine sandstone with greenish-gray mudstone
				90~280	Grey fine sandstone, siltstone interbedded with grey, dark grey mudstone, and silty mudstone
Paleozoic				0~225	Dense dark gray limestone, argillaceous limestone, calcareous dolomite, dolomitic limestone interbedded with quartz sandstone, gabbro, and basalt
Archaeozoic				0~750	Light red mixed granite

Based on the well logging data and the planar distribution of deposition facies, the porosity and permeability distributions of the target reservoir are plotted in Figure 4. It can be observed that both porosity and permeability are high. The average porosity and permeability in the oil-bearing formation are 31.2% and 2000 mD (mD = 10^{-15} m^2), and the average porosity and permeability in the water-bearing formation are 26.9% and 1300 mD. It should be noted that the oil layer is thick in the middle area but thin in the edge area of the reservoir. The physical property of oil is related to its distribution, and the oil viscosity in the middle area is about 500 cp, whereas the oil viscosity in the edge area is 1000 cp. Corresponding to the viscosity, the oil density in the middle area is 995 kg/m^3, but the oil density in the edge area is about 1000 kg/m^3.
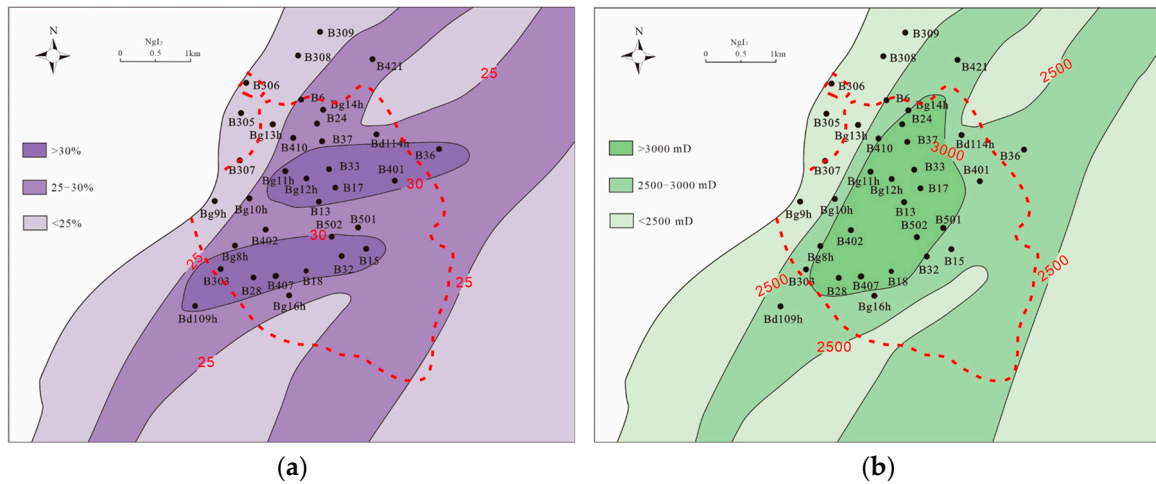
Figure 4. Distributions of porosity and permeability in the target reservoir (oil reservoir located within the red dotted line). (**a**) Porosity; (**b**) permeability.

2.5. Oil Migration Analysis

The NgI reservoir is located at the southern end of the Hainan tectonic belt, as shown in Figure 5, and there is only one major fault in the zone. The fault is a northeast-trending tensile fault with large fault spacing, long extension, and multiple stages. It controlled the oil and water distribution and accumulation in this area and provided a good channel for the early migration of oil and gas. According to the analysis of production data, the oil in the NgI reservoir comes from the lower formation along the fault.
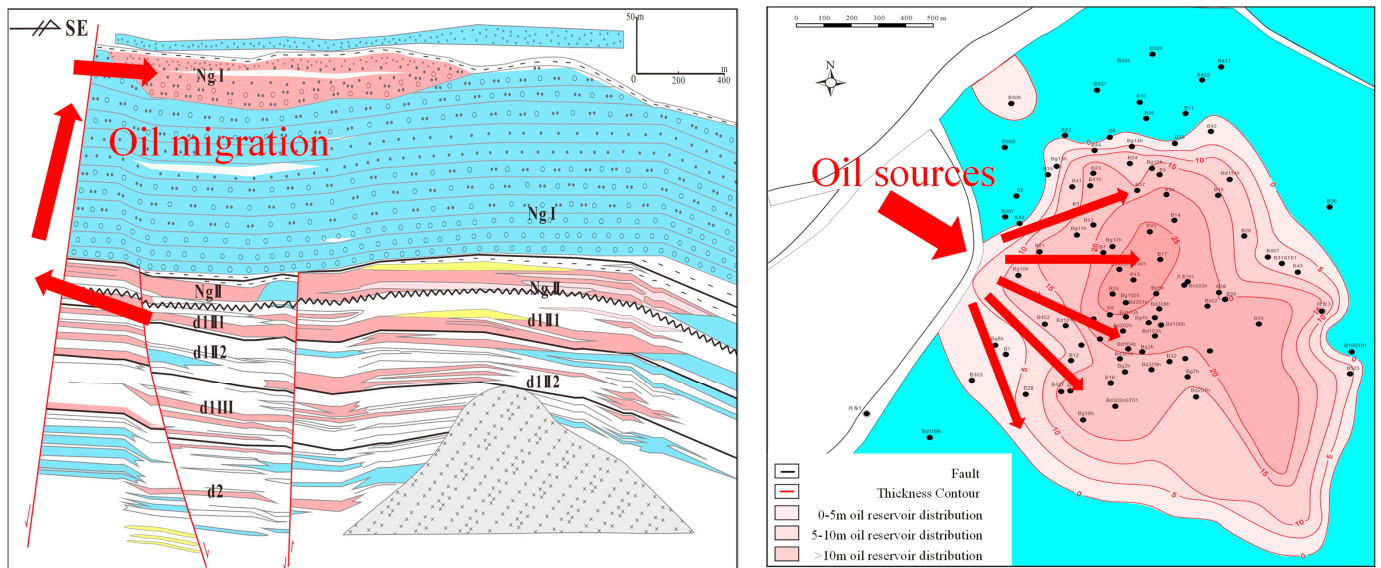

Figure 5. Oil migration and accumulation in the target reservoir.

As shown in Figure 5, oil migration in the Guantao Formation is mainly driven by subsequent oil migration, but the depth of the Guantao Formation is shallow, so the migration rate in the plane is small. There is a large amount of water in the Guantao Formation reservoir, and the moving oil inevitably comes into contact with the water. During the long-term contact between oil and water, the oil undergoes oxidation reactions, and the viscosity of the oil at the migration front becomes higher due to the oxidation reaction. After the viscosity increase in the oil at the migration front, the driving force is not enough to promote subsequent oil migration, so a lot of oil is gathered together and forms a reservoir with low viscosity in the middle and high viscosity at the edge.

3. Analysis of Current Production

In this section, the overall development status of the reservoir is first introduced, followed by an evaluation of the effectiveness of the existing steam huff and puff scheme based on the oil and water production data.

3.1. Overall Development Status

There are eight horizontal wells in the NgI reservoir, as shown in Figure 6, and they are Bn201h, Bn202h, Bn203h, Bn204h, Bn205h, Bn207h, Cn201h, and Cn202h. Four wells are located in the middle area with high oil saturation and slightly high oil viscosity, while the other four wells are located in the edge area with low oil saturation and high oil viscosity. The oil in the middle area can be exploited without steam injection, but the oil in the edge area only can be exploited by thermal recovery technology, especially, here, by steam huff and puff.
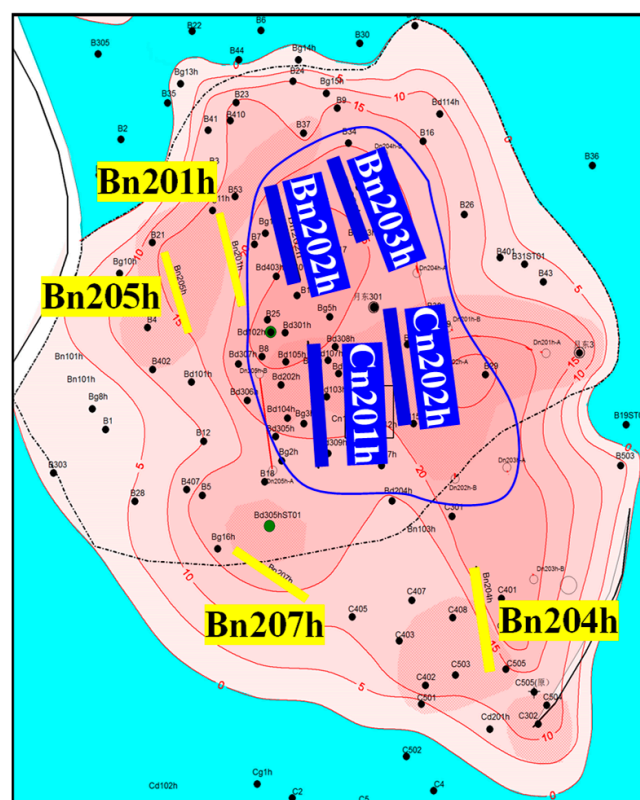

Figure 6. Well locations in the target reservoir (the background is the isopach, and the middle area of the reservoir is located in the blue circle, whereas the edge area is located outside the blue circle).

The reservoir has a geological reserve of 3.45 million tons, and the cumulative oil production is 35 thousand tons from 2020 to the end of 2022, with a recovery degree of 1.75%. As shown in Figure 7, the initial water cut is low with an average of 20%. However, with more and more wells in the edge area being opened to inject steam, the water cut increased to 60% at the end of 2021. At present, the daily fluid and oil production of the reservoir are 161.07 t/d and 62.57 t/d, respectively, and the average water cut is 61.20%. It can be predicted that the water cut will increase further in the future, so it is necessary to take more reasonable and advanced steam huff and puff measures to restrain the rise of water cut while maintaining oil production.
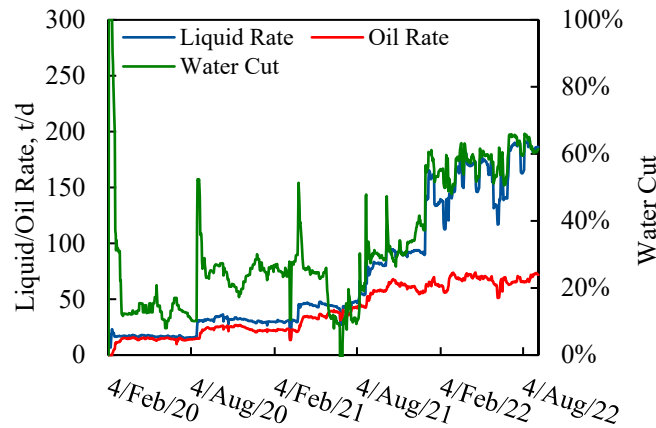
Figure 7. The liquid and oil production curves in the reservoir.

3.2. Oil and Water Production

3.2.1. Middle Area

In the middle area of the reservoir, the oil saturation is high, but viscosity is relatively low, so the oil can be exploited for 2 years or more for the four wells without steam injection. By the end of 2022, 28 thousand tons of oil have been produced with an average oil recovery of 0.85%. It can be seen from the production dates shown in Figure 8 that the liquid production rate is controlled below 20 t/d and the oil production rate remained around 12 t/d before August 2021. However, after the liquid production rate increased to 23 t/d, the average oil production rate continued to decline and fall to 9% at the end of 2022. It can be inferred that increasing the liquid rate would aggravate the bottom water intrusion, so the liquid production rate should be controlled below 20 t/d.
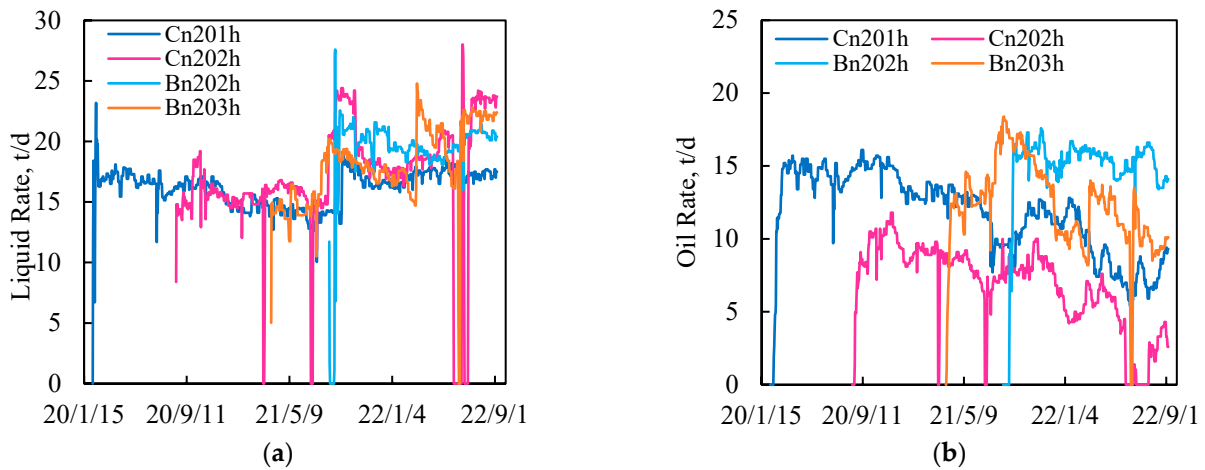

Figure 8. The liquid and oil production curves in the middle area of the reservoir. (**a**) Liquid production curve; (**b**) oil production curve.

Generally, the oil in the middle area can be exploited steadily for about 1 year due to the high oil saturation and relatively low viscosity. However, with the continuation of production, the water cut increases quickly due to the bottom water invasion, as shown in Figure 9. For example, Cn201 was the first well to exploit oil, and its water cut was lower than 20% for a long time, but the water cut rose rapidly in a stepped shape after 500 days of exploitation. The water cut in Well Bn203h shows a similar variation, but it increased from 20% to 60% only in a short time. Therefore, it can be judged that the water cut in Well Bn202h will go through a similar variation, even though Well Bn202h began operation recently.
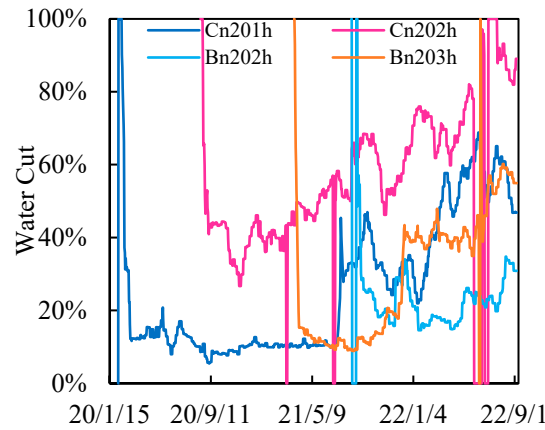
Figure 9. The water cut curve in the middle area of the reservoir.

3.2.2. Edge Area

In the edge area of the reservoir, the oil saturation and viscosity are high, so the steam huff and puff are adopted to exploit the oil at the beginning. The steam injection rate is controlled in the range of 100–300 t/d, and the steam quality is about 0.7. The cyclic steam injection volume is about 1000 t, and the liquid production rate is controlled at about 25 t/d. By the end of 2022, the cumulative oil production is about 7 thousand tons, and the oil recovery is only 0.2% due to the short exploitation time. Although the steam huff and puff can reduce water cut and increase the oil production rate in a short time, the overall oil production rate still declines slowly due to the strong effect of the edge and bottom water. To maintain the stability of the oil production rate, the average liquid production rate was slowly increased from the initial 20 t/d to the current 30 t/d, as shown in Figure 10.
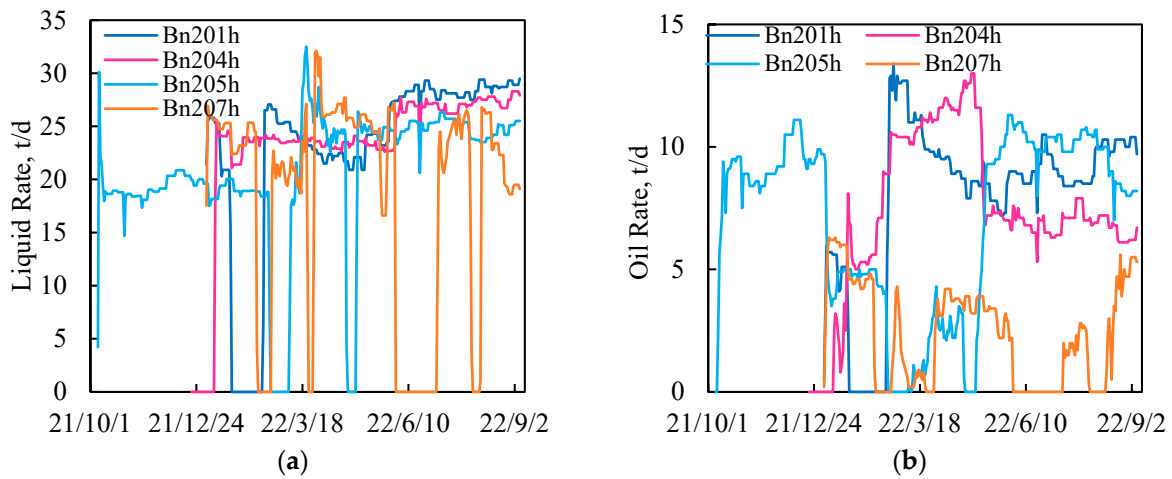

Figure 10. The liquid and oil production curves in the edge area of the reservoir. (**a**) Liquid production curve; (**b**) oil production curve.

Generally, the steam huff and puff can exploit heavy oil in the edge area, but the water cut continues to rise with the increase in steam cycles, as shown in Figure 11. For example, Wells Bn204h and Bn205h can exploit oil for a period of time after the first cycle of steam huff and puff, but the water cut rises to about 80% quickly due to the bottom water invasion. After the second cycle of steam huff and puff, the water cut decreases to about 6%. For Well Bn201h, a similar variation of water cut occurs, and the stream huff and puff only works for three months. However, because the area in which Well Bn207h is located is thin, the bottom water has a great influence on the oil production. The water cut in Well Bn207h is always above 80%, and sometimes, it increases to above 90%. Even the steam huff and puff makes it hard to reduce the water cut.
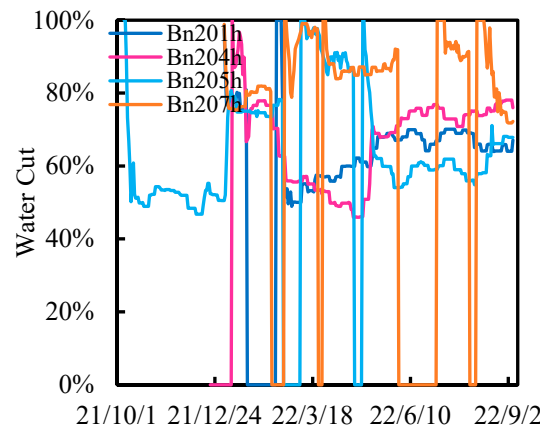
Figure 11. The water cut curve in the edge area of the reservoir.

3.3. Current Evaluation

It can be seen from the above analysis that whether thermal recovery is adopted or not, the thinner the reservoir thickness, the higher the bottom water ridging rate and the faster the water cut rise. Therefore, as shown in Figure 12, the production process of the bottom water heavy oil reservoirs can be divided into three stages: stable oil production, local bottom water intrusion, and expansion of bottom water intrusion. Because the density difference between oil and water is small, the oil is mainly displaced by the local pressure drop around the well in the beginning. Subsequently, the pressure drop travels rapidly to the bottom water, and the bottom water migrates upward into the well and forms local bottom water intrusion. Lastly, as the bottom water continues to flow upward, the weep region of the bottom water expands and results in rapid water invasion. Notably, the thinner the reservoir thickness and the higher the viscosity of the crude oil, the higher the water cut rise rate of the production well.
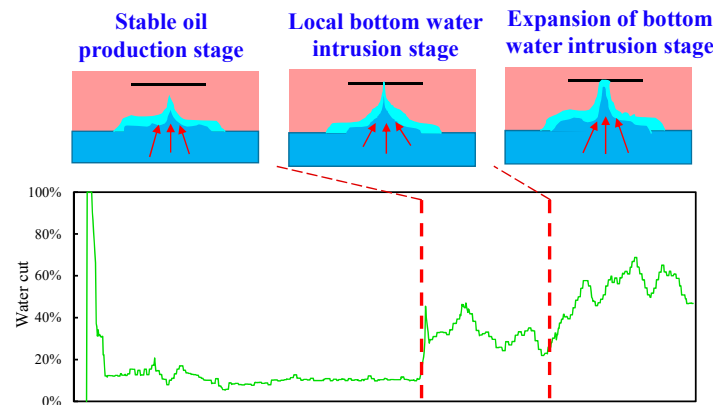

Figure 12. Sketch map of bottom water intrusion process.

After a long period of oil exploitation in the middle area, the average water cut has reached about 60%, and it will transform from the stable oil production stage to the local bottom water intrusion stage. Although the average water cut in the middle area is lower than that in the edge area, its rising rate is higher, so it is necessary to take certain measures or changes to reduce the further rise of the water cut. The steam huff and puff is a good choice, but its effect needs further evaluation. A preliminary test has been conducted in Well Bn207h, but its water cut rises faster, so whether the middle area should adopt steam huff and puff is still questionable.

For the edge area, the steam huff and puff measures can stabilize the water cut, generally. For example, as shown in Table 2, after a steam injection of 1055 t into Well Bn201h, the water cut reduced from 78% to 54%. After a steam injection of 1215 t into

Bn205h, the water cut reduced from 89% to 59%. However, the effect of steam huff and puff on water reduction is not obvious in some wells. For example, after a steam injection of 1105 t into Well Bn207, the water cut still increased, but it reduced by 5% only with an increase in the steam injection volume to 1864 t. Therefore, it can be seen that the current parameters of steam huff and puff still need to be optimized in combination with the accurate geological model.

Table 2. Water and oil production changes after steam huff and puff.

Well	Steam Injection Parameter			Production Parameter before Steam Huff and Puff			Production Parameter after Steam Huff and Puff		
	Cyclic Steam Injection, t	Steam Quality, %	Steam Injection Rate, t/h	Liquid, t/Day	Oil, t/Day	Water Cut, %	Liquid, t/Day	Oil, t/Day	Water Cut, %
YD-Cn202h	1000	69.6	12.9	19.9	4.0	79.9	23.6	2.6	89
YD-Bn201h	1055	65.7	12.9	22.4	5.0	77.7	24	11	54.2
YD-Bn205h	1215	72.5	13.8	24.3	2.7	88.9	23.7	9.5	59.9

4. Geological and Simulation Models

4.1. Geologic Modeling

Based on reservoir logging and core data, a 3D geological model of the target reservoir was established [30]. The three-dimensional geological structure and sedimentary facies of the reservoir were established first, and then, the distributions of porosity, permeability, and oil saturation were generated using Sequential Gaussian Simulation [31]. To verify the reservoir's physical parameters and the oil distribution in the geological model, as shown in Figure 13, the volume calculation module was used to calculate the oil reserve, and the obtained reserve is 3.55 million tones, which is the same as the petroleum-in-place.
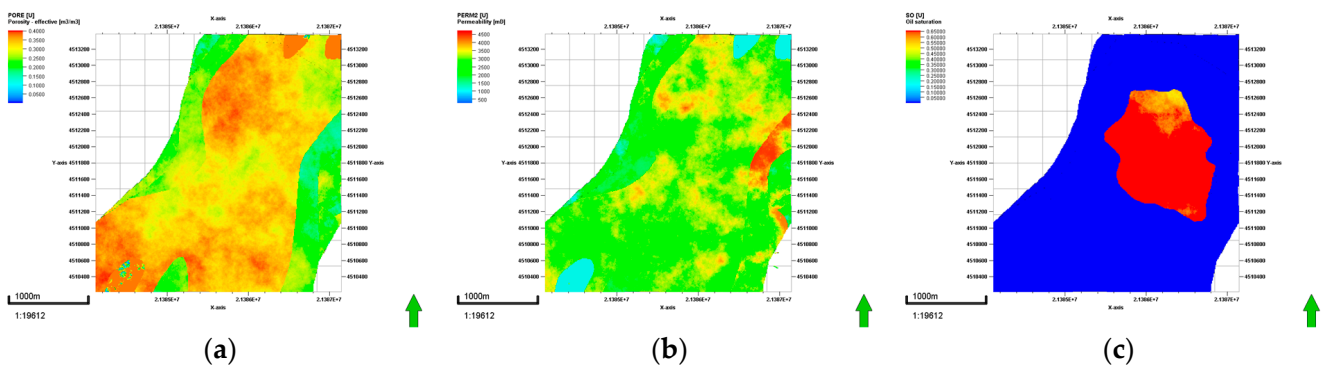

(**a**)　　　　　　　　(**b**)　　　　　　　　(**c**)

Figure 13. Distributions of porosity, permeability, and oil saturation in the geological model. (**a**) Porosity; (**b**) permeability; (**c**) oil saturation.

4.2. Simulation Model and History Matching

It is necessary to establish an accurate simulation model to accurately predict the subsequent oil and water production. To this end, we first reduced the meshes of the geological model to $400 \times 400 \times 10$ using grid coarsening technology, then it was imported into reservoir numerical simulation software, CMG (https://www.cmgl.ca/solutions/software/gem/ accessed on 15 June 2024). The current grid size can ensure the accuracy of the simulation result and the operation efficiency, at the same time. Subsequently, the well trajectory, perforation, production, and steam huff and puff data were written and imported into the software for historical fitting and analysis.

Water, oil, N_2, and CO_2 were added to the model before performing the historical matching, and their properties are shown in Table 3. Under the reservoir condition, the density of crude oil is 0.9930~0.9949 g/cm^3, and its viscosity ranges from 500 to 1000 cp. According to the parameters of oil samples and geological analysis, the oil viscosity in the edge area is higher than that in the middle area of the reservoir, so we set the oil viscosity in the edge area to 1000 cp and the oil viscosity in the middle area to 500 cp. The viscosity values of crude oil with a viscosity of 500 cp at different temperatures are shown in Figure 14, and the viscosity–temperature curve of 1000 cp of crude oil increases in proportion to the viscosity ratio. Subsequently, the initial relative permeability curves provided by the oil company were imported into the software, and the final relative permeability curves were obtained by constantly adjusting them to match the field production data, as shown in Figure 14.

Table 3. Key parameters of the base case model.

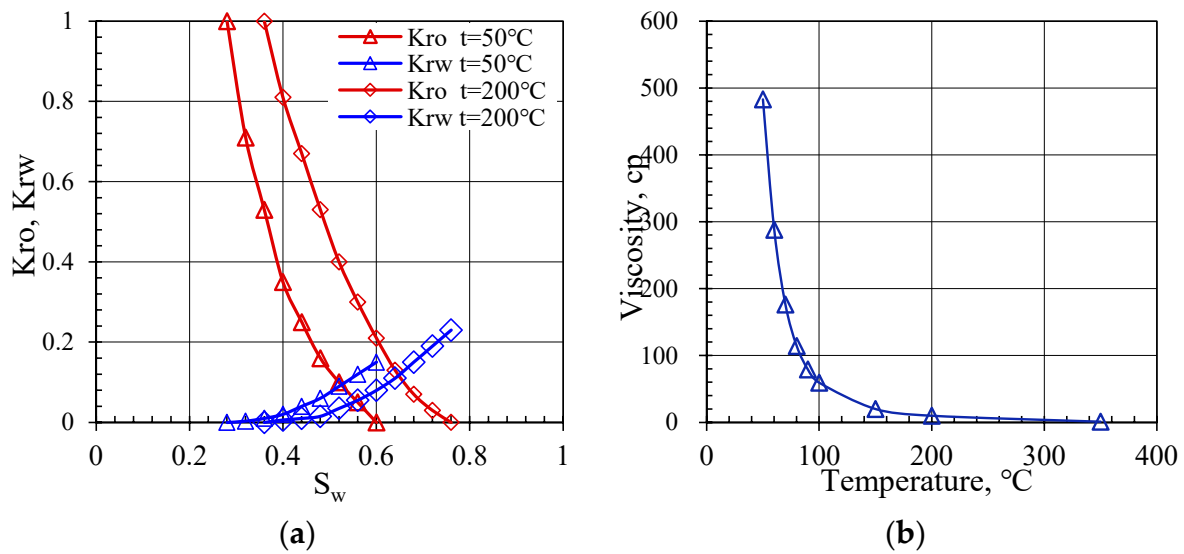| Parameters	Density at Standard Condition	P_{Crit}, MPa	T_{Crit}, C	Compressibility, 1/kPa
Water	1000	22.12	374.15	5×10^{-7}
Oil	995	0	0	3×10^{-6}
N_2	1.142	3394	−146.95	-
CO_2	1.803	7.53	31.05	-

Figure 14. Relative permeability and viscosity curves used in the simulation model. (**a**) Relative permeability curves under different temperatures; (**b**) viscosity curve under different temperatures.

Different from previous historical matching, there is no uniform oil–water contact in the longitudinal direction, so it is necessary to modify the oil–water interface through the multiple history matching of the whole reservoir, single wells, and the whole reservoir again. Firstly, the data of cumulative oil and water production data in the whole reservoir were matched by adjusting the relative permeability curves, as shown in Figures 15 and 16. Subsequently, the oil and water production data in every well were matched by adjusting the bottom interface of oil and water. Lastly, the modified bottom interface of oil and water in every single well was re-assigned to the whole geological model, and the whole reservoir history matching was conducted again by adjusting the relative phase curves finely.
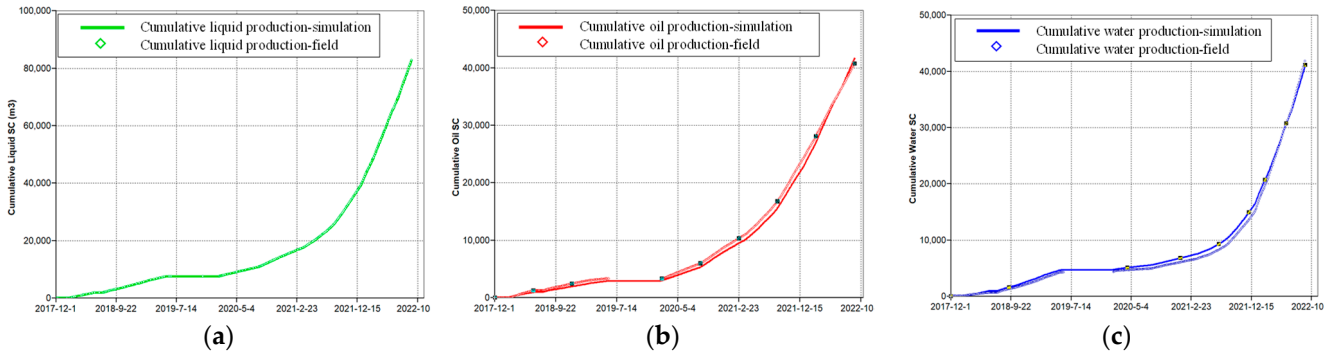
Figure 15. History matching of cumulative oil and water production. (**a**) Cumulative liquid; (**b**) cumulative oil; (**c**) cumulative water.
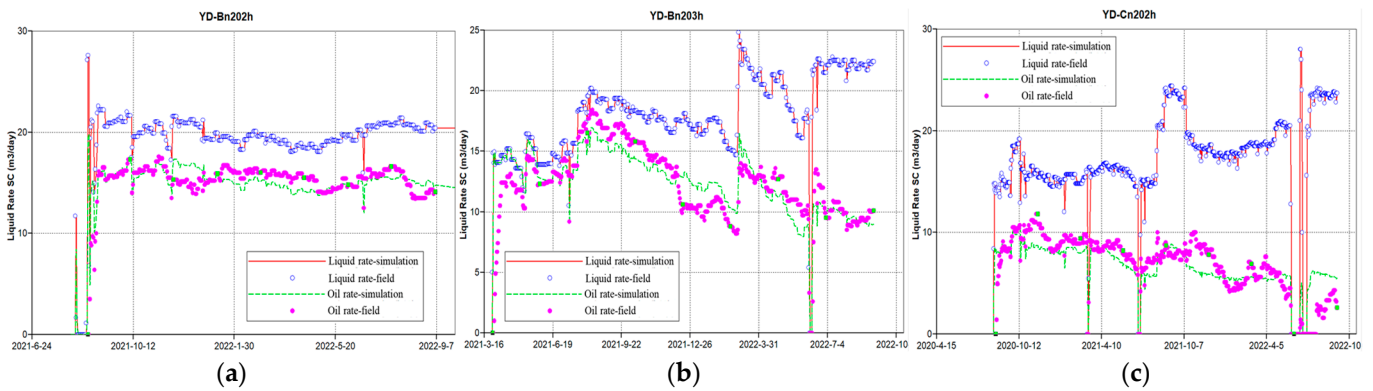

Figure 16. History matching of some typical wells. (**a**) Well Bn202h; (**b**) Well Bn203h; (**c**) Well Cn202h.

4.3. Residual Oil Distribution

Generally, the oil saturation in the plane does not change much, as shown in Figure 17. Only the oil saturation in the area around the production well decreases due to bottom water invasion, and the residual oil is mainly distributed in the interval of horizontal wells. Notably, the residual oil distribution is mainly controlled by the production parameters and the vertical location of each well. For the middle area, although the thickness is high, the high pressure drop caused by long-term exploitation leads to bottom water invasion, resulting in a decrease in oil saturation around the well. For the edge area, because oil pay thickness and saturation are low, the bottom water invades upward quickly and results in a decrease in oil saturation around the horizontal well.
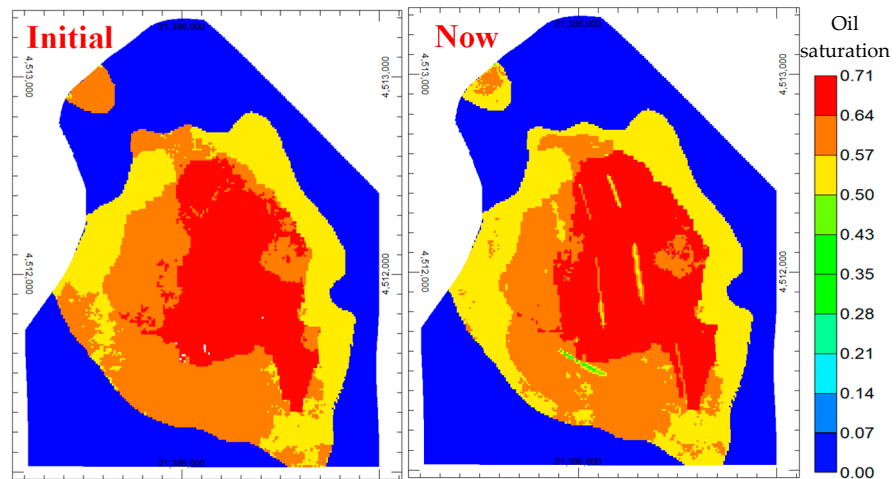

Figure 17. The initial and current oil saturation distributions in the reservoir.

The detailed oil saturation in the vertical direction can be seen in Figure 18. Generally, the residual oil is mainly located in the area above the horizontal wells and the area between the horizontal wells. Wells Cn201h and Cn202h are taken as typical examples for the middle area. The initial oil saturation around these wells is high, but the oil below the wells is displaced by the bottom water after 2 years of exploitation. Well Bn207h is taken as a typical example for the edge area, and the oil saturation around the well decreases due to the bottom water invasion after 1 month of exploitation.
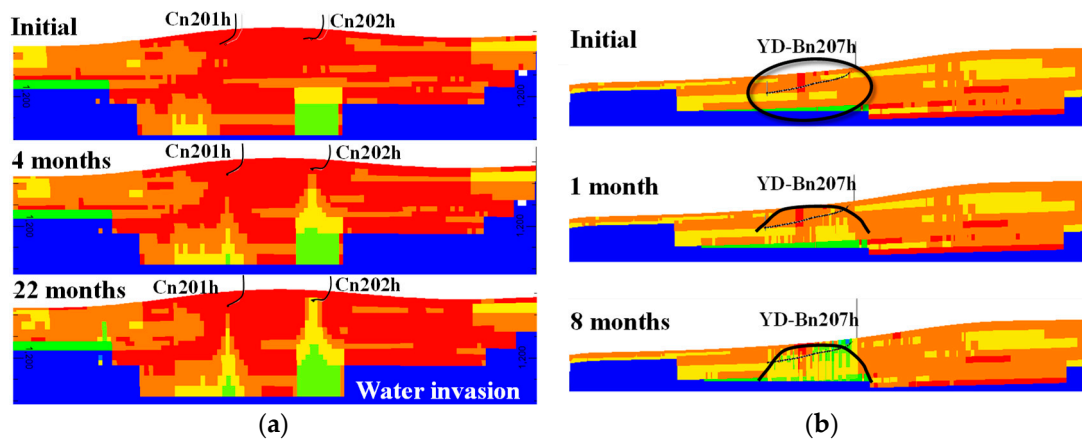

(a) (b)

Figure 18. The change of oil saturation distribution in the vertical dimension. (**a**) Wells Cn201h and Cn202h in the middle area; (**b**) Well Bn207h in the edge area.

5. Exploitation Scheme Design

The oil recovery effect of steam huff and puff in some areas is good, while in others, it is not good, so the conventional steam huff and puff development recovery method in onshore heavy oil cannot be copied directly. Based on the above analysis of reservoir type and production, the exploitation scheme of this type of offshore reservoir is mainly related to its viscosity distribution and one bottom oil–water contact. In the edge area of the reservoir, the oil viscosity and bottom water energy are high, steam huff and puff can be adopted to increase oil production and reduce water invasion. During the steam huff and puff, the bottom water invasion rate should be slowed down by controlling the cyclic steam injection volume, but at the same time, the bottom water should be used to displace more oil. In the middle area of the reservoir, the oil viscosity and bottom water energy are low, oil can be exploited without steam injection, and the steam huff and puff may be considered after the water cut increases to a high value. To this end, we first optimized the steam injection parameters based on the single well model in the edge area, and then analyzed the liquid production rates in the middle region to design the oil exploitation scheme.

5.1. Steam Huff and Puff Optimization

5.1.1. Steam Injection Parameters

Firstly, the Bn207 single well model is extracted from the above geological model to analyze and optimize the steam injection parameters. The cyclic steam injection volume per unit length (the length of the horizontal interval in Bn207 is 250 m) is changed from 2, 4, 6, and 8, to 10 t/m to analyze its effect on oil production. It can be seen from Figure 19 that the cyclic oil production volume firstly increases and then decreases with the increase in the cyclic steam injection volume. This is because the injected steam can contact the bottom water when the steam injection volume is too high. Therefore, 1500 tons of steam is suggested to be injected into to the reservoir due to the highest cyclic oil production volume. Considering the variation of reservoir thickness, the optimal cyclic steam injection volume may be different, so the optimizations in Wells Bn201 and Bn204 are also analyzed, and the results are shown in Figure 20. It can be seen that the optimal cyclic steam injection volume is different in different regions, and the thicker the reservoir, the higher the cyclic

steam injection volume. If the value of dividing the cyclic steam injection volume per unit length by the reservoir thickness is adopted to express the optimal steam injection in each well, it is about 0.4 t/(m·m) for the entire reservoir.
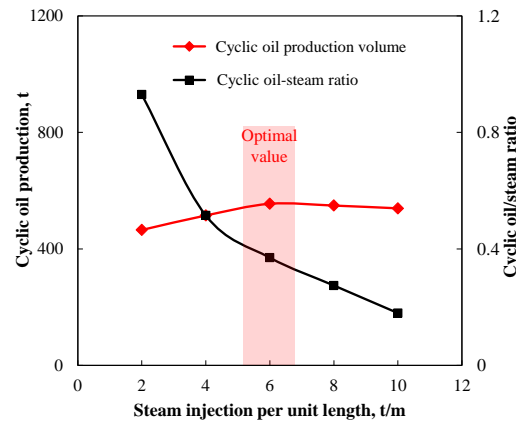

Figure 19. Cyclic oil production under different cyclic steam injections.
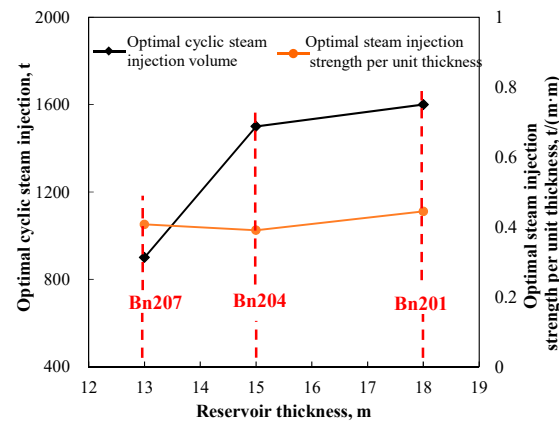

Figure 20. Optimal steam injection under different reservoir thicknesses.

The steam injection rate is changed from 100, 200, 300, 400, and 500, to 600 t/day to analyze its effect on the oil production. Because the bottom steam quality changes with the steam injection when the well top steam quality is 0.75, the values of steam quality under different steam injection rates are also considered in the analysis. It can be seen from Figure 21 that cyclic oil production volume increases rapidly with the increase in the steam injection rate when the steam injection rate is lower than 400 t/d, and then it increases slowly. Theoretically, a higher steam injection rate is suggested under the constant steam quality at the well top, but reservoir pressure rise and injection pump limits constrain high steam injection rate in the field application, so the 400 t/d of steam injection rate is chosen in the reservoir.

The cyclic steam injection volume should be increased to expand the heating radius around the well, as the steam huff and puff cycle increases. In order to optimize the increase rate of cyclic steam injection volume with the increase in cycles, the cumulative oil production in the next ten years is taken as the objective function, and the steam injection volume per cycle is increased by 10%, 20%, and 30%, respectively, to analyze their effect on the objective function. The results are shown in Figure 22, and it can be seen that the cumulative oil production increases with the increase in cyclic steam injection volume when the increase rate of cyclic steam injection volume is less than 10%. However, the cumulative oil production decreases with the increase in cyclic steam injection volume when the increase rate of cyclic steam injection volume is higher than 10%. Therefore, the optimal increase rate of cyclic steam injection volume is 10%.
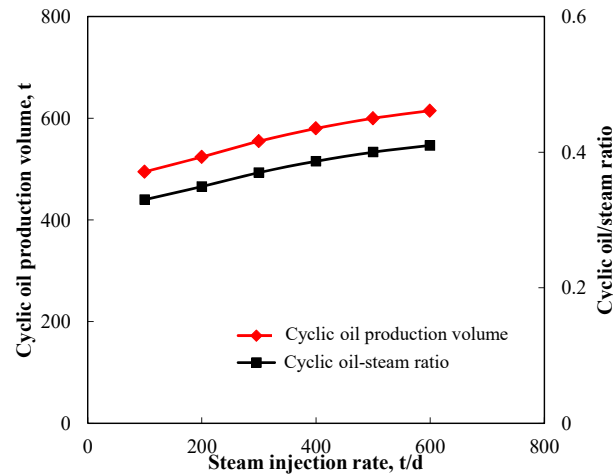
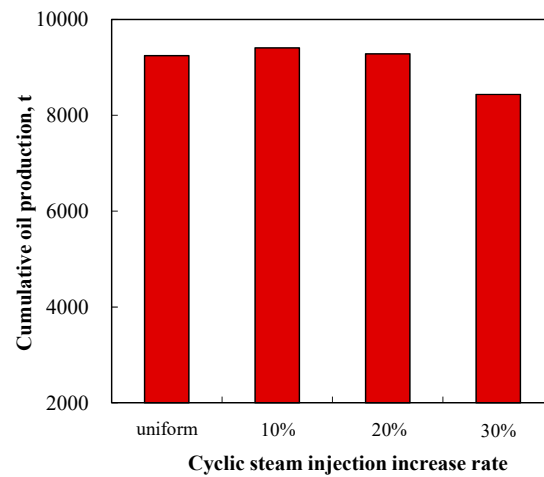**Figure 21.** Cyclic oil production under different steam injection rates.

Figure 22. Cumulative oil production under different steam injection increase rates.

5.1.2. N_2-Assisted Steam Huff and Puff

Based on the optimized parameters in steam huff and puff, N_2 [32] was co-injected with steam in subsequent different steam huff and puff cycles [33–35], and the cyclic oil increment and oil–steam ratio were analyzed compared with the pure steam huff and puff. It can be seen that the earlier N_2 co-injection can increase oil production and oil–steam ratio, so the N_2 may be suggested to be co-injected with steam in the latest cycle. The oil increment and oil–steam ratio under different N_2 injection volumes are analyzed, and the results are shown in Figure 23. The oil increment increases with the increase in the injected N_2, but the rising trend slows down, gradually. However, it is found that when the N_2 injection amount is 5000 m^3, the oil increment per unit volume of N_2 is the highest. Therefore, when the ratio of N_2 to steam is about 3.5, N_2 has the best effect on water invasion inhibition and oil increment.

The process of water invasion inhibition caused by N_2 injection can be seen in Figure 24. After the N_2 injection, the water around the well is displaced by the injected N_2 and the subsequent injected steam can contact the crude oil directly. Although part of the injected N_2 is produced in the well during steam puff, a large amount of N_2 remains at the top of the reservoir, which plays the role of maintaining the reservoir pressure and displacing the residual oil.
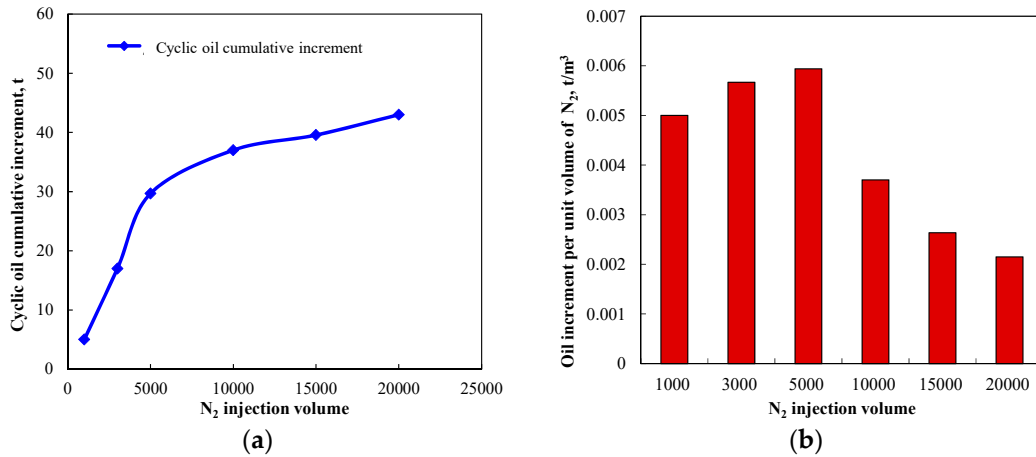
Figure 23. The cyclic oil increments and oil–steam ratios under different N_2 co-injection rates. (**a**) Cyclic oil increment; (**b**) oil/N_2 ratio.
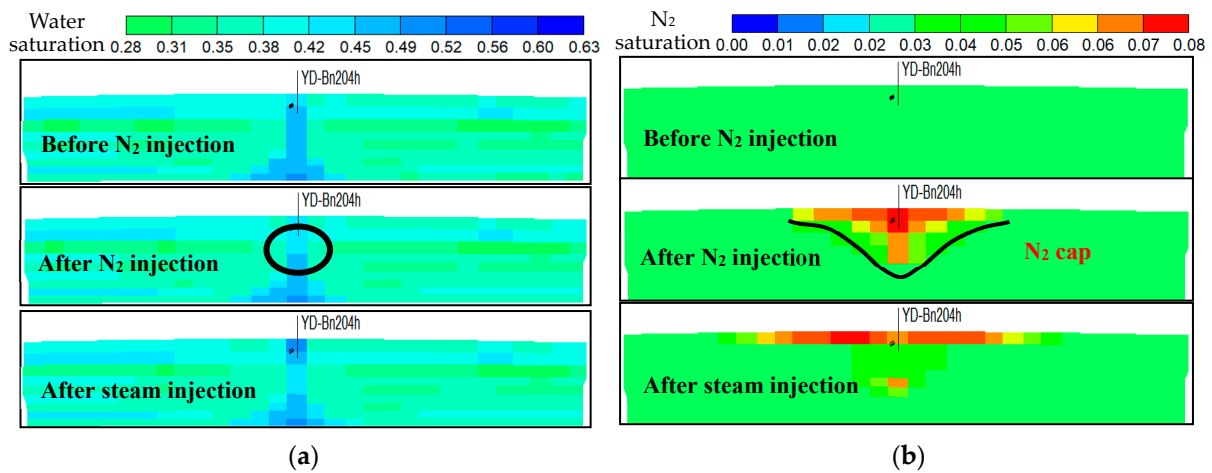

Figure 24. The distributions of water saturation and N_2 under different times. (**a**) Water saturation distributions; (**b**) N_2 distributions.

5.1.3. CO_2-Assisted Steam Huff and Puff

Previous studies have shown that CO_2-assisted steam huff and puff can effectively reduce the viscosity of heavy oil [36,37], improve oil production, and maintain the pressure at the late stage [38–40]. In this section, the cyclic oil increment and oil–steam ratio under different CO_2 injection volumes are analyzed, and the results are shown in Figure 25. Similar to N_2, the oil increment increases with the increase in injected CO_2, but the rising trend slows down, gradually. This is because the oil expansion caused by CO_2 dissolution is dominant when the injected CO_2 amount is small, and the oil increment increases with the increase in injected CO_2. However, with the continuous increase in CO_2, the injected CO_2 would push oil away from the well, and hence, the oil increment slows down. Therefore, when the CO_2 injection amount is 3000 m^3 (i.e., ratio of CO_2 to steam is 2), the oil increment per unit volume of CO_2 is the highest.

Similar to N_2, CO_2 injection can displace the formation water away from the well and improve the reservoir pressure. However, different from N_2, a large amount of the injected CO_2 dissolves into the crude oil and does not move up to the reservoir top under gravity, as shown in Figure 26. Therefore, excessive CO_2 injection may reduce the viscosity of the heavy oil around the well, but it may push the oil to the bottom oil–water contact and lead to a negative impact on oil production. The specific mechanism of water inhibition and improved oil recovery of CO_2 and N_2 are different, and N_2 and CO_2 can be combined to simultaneously reduce oil viscosity and maintain reservoir top pressure in the future.
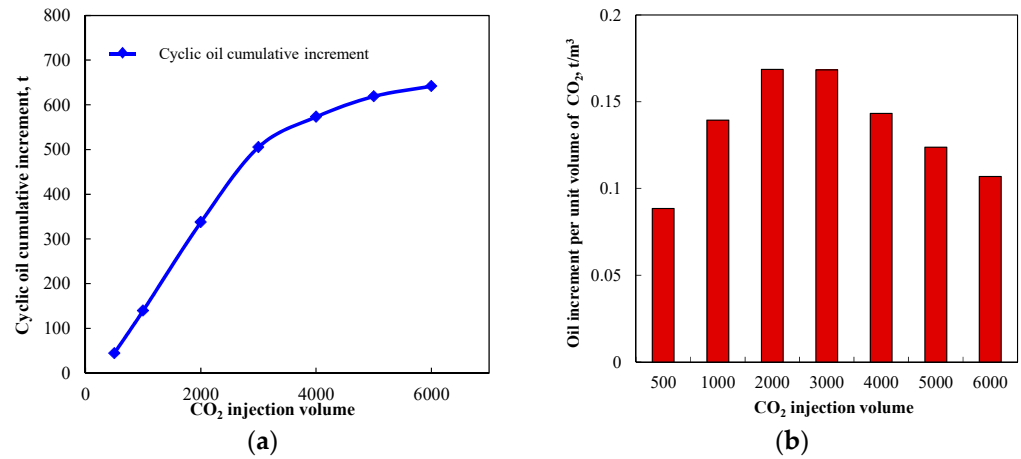
Figure 25. The cyclic oil increments and oil–steam ratios under different CO_2 co-injection rates. (**a**) Cyclic oil increment; (**b**) oil–steam ratio.
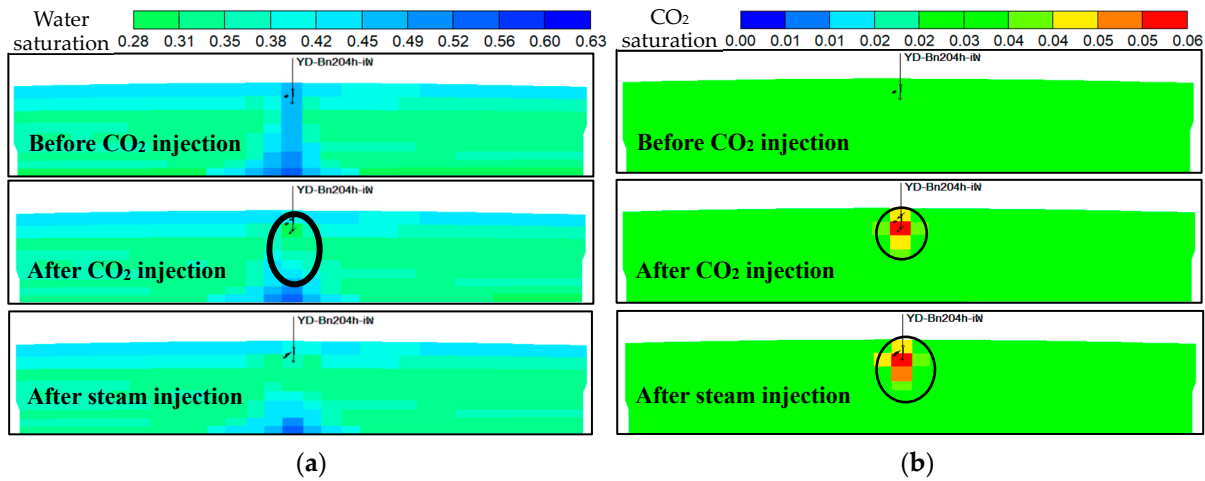

Figure 26. The distributions of water saturation and CO_2 at different times. (**a**) Water saturation distributions; (**b**) CO_2 distributions.

5.2. Exploitation Optimization and Production Forecast

Based on the above production analysis and the steam huff and puff optimization, the exploitation schemes of the target reservoir in the next ten years were designed as shown in Table 4. The steam huff and puff is adopted in the edge area, but the oil in the middle area is exploited without steam injection. For the wells in the edge area, the cyclic steam injection volume per unit length is set to the product of 0.4 t/(m·m) and the reservoir thickness, the steam injection rate is set to 400 t/d, and the liquid production rate is set to 20 m³/d. For the wells in the middle area, the liquid production rate is set to 5, 10, 20, 30, and 40 t/day to analyze their effect on the oil production in the whole reservoir. Also, the N_2- and CO_2-assisted steam huff and puff are also considered to analyze their effect on cumulative oil production.

Figure 27 shows the cumulative oil production in different exploitation schemes. It can be seen that when the production rate in the middle area is lower than 20 t/day, the cumulative oil production increases with the increase in the production rate. When the production rate in the middle area is higher than 20 t/day, the bottom water intrusion rate increases due to the high pressure drop, so the cumulative oil production decreases with the increase in the liquid production rate. Therefore, the recommended liquid production rate ranges from 15 to 25 t/day, and the optimal liquid production rate is about 20 t/day for the middle area. The N_2 and CO_2 injection can only increase the cumulative oil production by 2% and 5%, so these assistant gases are not to be injected with steam after considering

the economic cost. Figure 28 shows the curves of cumulative liquid production, cumulative oil production, and water cut in the next ten years in case 3, and the residual oil distribution is also shown after 10 years of exploitation.

Table 4. Parameters in different exploitation schemes.

Case	Parameters in Steam Huff and Puff in the Edge Area				Parameters in the Edge Area
	$\tau,/(\text{m·m})$	Steam Injection Rate, t/Day	Assistant Gas	Liquid Production Rate, t/Day	Liquid Production Rate, t/Day
1	0.4	400		20	5
2	0.4	400	-	20	10
3	0.4	400	-	20	20
4	0.4	400	-	20	30
5	0.4	400	-	20	40
6	0.4	400	N_2	20	20
7	0.4	400	CO_2	20	20

Note: τ is the value obtained by dividing the cyclic steam injection volume per unit length by the reservoir thickness.
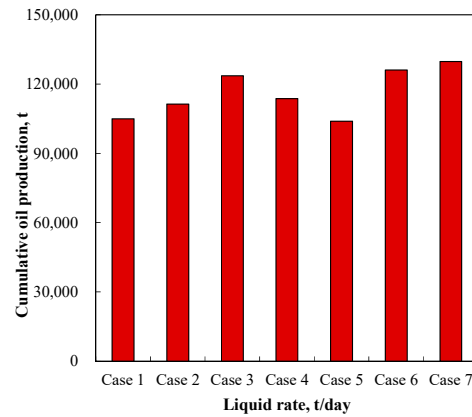

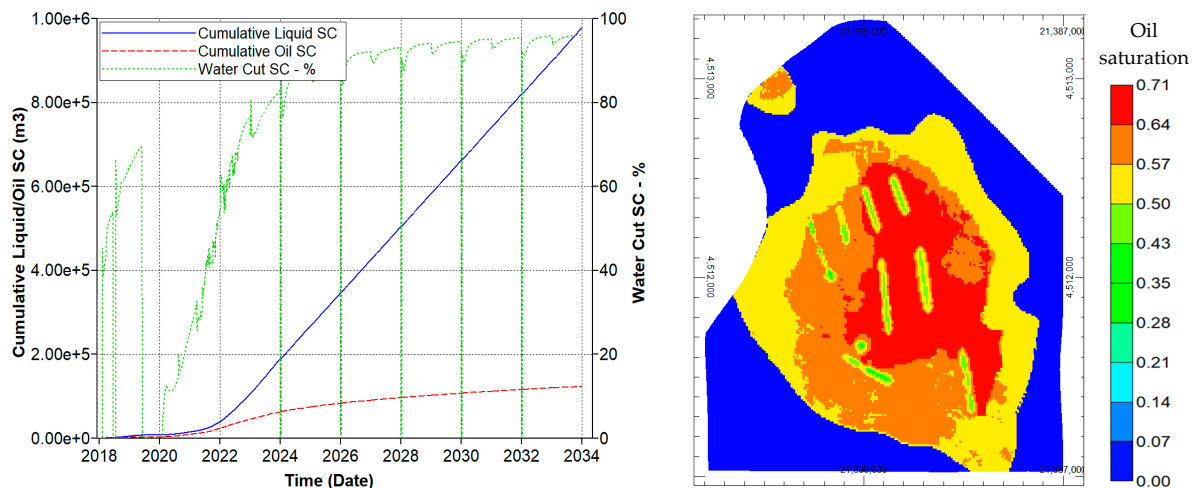**Figure 27.** Cumulative oil productions under different exploitation schemes.

Figure 28. Cumulative production curves and residual oil distribution after 10 years of exploitation in case 3.

6. Conclusions

(1) The oil in the NgI reservoir comes from the lower formation along the fault, and the migrated oil contacts with groundwater for a long time due to insufficient force. During the long-term contact between oil and water, the oil undergoes oxidation

reactions, and the viscosity of the oil at the migration front becomes higher due to the oxidation reaction. Combined with the abundant edge and bottom water, the reservoir may be identified as a self-sealing bottom water heavy oil reservoir.

(2) The oil viscosity in the middle area is high while the oil viscosity in the edge area is relatively low, so the steam huff and puff was adopted to exploit oil in the edge area. Although the water cut in the middle area has risen to about 60% after a long period of oil exploitation without steam injection, the effect of steam huff and puff on oil increment is not obvious. At present, the cyclic steam injection volume in the edge area is controlled at about 1000 tons, which can barely achieve stable oil production. However, the oil production can be maintained only by increasing the cyclic steam injection volume in some wells in the edge area. Therefore, the current parameters of steam huff and puff still need to be optimized in combination with the accurate geological model.

(3) Generally, whether steam huff and puff is adopted or not, the thinner the reservoir thickness, the higher the bottom water invasion rate and the faster the water cut rise, so it is crucial to identify the accurate bottom oil–water contact. To this end, based on the existing seismic and logging data, we re-corrected the oil–water boundary at the bottom of the reservoir through a reduplicative history matching of wells and reservoir, and then established a 3D reservoir geological model. This geological modeling method with accurate oil–water contact can be extended to other oil reservoirs.

(4) All of these kinds of offshore heavy oil reservoirs can be developed by a combination of thermal production and cold production. The specific production and steam injection values depend on the specific reservoir condition, and more importantly, the cyclic steam injection volume should be designed after considering the reservoir thickness. For this case study, the value of dividing the cyclic steam injection volume per unit length by the reservoir thickness is suggested to be 0.4 t/(m·m). The steam injection rate is set to 400 t/d, and the liquid production rate is set to 20 m^3/d. The optimal exploitation scheme predicts that 84 thousand tons of oil could be exploited by 2034.

References

1. Yu, L.D. The distribution of the world's heavy oil resources and the status quo and prospects of their exploitation technologies. *Spec. Oil Gas Reserv.* **2001**, *8*, 98–103.
2. Sun, H.; Liu, H.; Wang, H.; Shu, Q.; Wu, G.; Yang, Y. Development technology and direction of thermal recovery of heavy oil in China. *Acta Pet. Sin.* **2022**, *43*, 1664–1674.
3. Dong, X.; Liu, H.; Hou, J.; Zhang, Z.; Chen, Z. Multi-thermal fluid assisted gravity drainage process: A new improved-oil-recovery technique for thick heavy oil reservoir. *J. Pet. Sci. Eng.* **2015**, *133*, 1–11. [CrossRef]
4. Wang, Y. Air Injection Assisted Cyclic Steam Stimulation Process for Enhanced Ultra Heavy Oil Recovery. Ph.D. Thesis, China University of Petroleum, Qingdao, China, 2020.
5. Cui, G.; Liu, T.; Xie, J.; Rong, G.; Yang, L. A review of SAGD technology development and its possible application potential on thin-layer super-heavy oil reservoirs. *Geosci. Front.* **2022**, *13*, 101382. [CrossRef]
6. Pei, S.; Cui, G.; Wang, Y.; Zhang, L.; Wang, Q.; Zhang, P.; Huang, L.; Ren, S. Air assisted in situ upgrading via underground heating for ultra heavy oil: Experimental and numerical simulation study. *Fuel* **2020**, *279*, 118452. [CrossRef]

7.   Hemmati-Sarapardeh, A.; Alamatsaz, A.; Dong, M.; Li, Z. *Thermal Methods*; Gulf Professional Publishing: Houston, TX, USA, 2023.
8.   He, H.; Li, Q.; Zheng, H.; Liu, P.; Tang, J.; Ma, Y. Simulation and evaluation on enhanced oil recovery for steam huff and puff during the later phase in heavy oil Reservoir—A case study of block G in Liaohe oilfield, China. *J. Pet. Sci. Eng.* **2022**, *219*, 111092. [CrossRef]
9.   Liu, P.; Zhang, Y.; Liu, P.; Zhou, Y.; Qi, Z.; Shi, L.; Xi, C.; Zhang, Z.; Wang, C.; Hua, D. Experimental and numerical investigation on extra-heavy oil recovery by steam injection using vertical injector-horizontal producer. *J. Pet. Eng.* **2021**, *205*, 108945. [CrossRef]
10.   Dong, X.; Liu, H.; Chen, Z.; Wu, K.; Lu, N.; Zhang, Q. Enhanced oil recovery techniques for heavy oil and oilsands reservoirs after steam injection. *Appl. Energy* **2019**, *239*, 1190–1211. [CrossRef]
11.   Pan, G.; Wu, J.; Zhang, C.; Li, H.; Liu, D. Oil enhancement analysis of weak-gel-assisted soak in offshore heavy oil reservoir. *Spec. Oil Gas Reserv.* **2017**, *24*, 134–138.
12.   Cheng, D. Recovery Countermeasures and Potential Indicators of Horizontal Well in Commination Well Pattern. *Spec. Oil Gas Reserv.* **2019**, *26*, 88–92.
13.   Wang, T.; Liu, F.; Li, X. Optimization of Efficient Development Modes of Offshore Heavy Oil and Development Planning of Potential Reserves in China. *Water* **2023**, *15*, 1897. [CrossRef]
14.   Zhang, H.; Liu, P.; Wang, Q.; Bai, J.; Zhang, W.; Zhang, H.; Han, X. Artificial Lift System Applications for Thermally Developed Offshore Heavy Oil Reservoirs. In Proceedings of the Offshore Technology Conference Asia, Virtual and Kuala Lumpur, Malaysia, 22–25 March 2022.
15.   Li, L.; Yang, J.; Zou, X.; Jia, L.; Zhang, C.; Wang, Q. A new production string for improving the thermal recovery of offshore heavy oil in small block reservoirs. *J. Pet. Sci. Eng.* **2022**, *211*, 110131. [CrossRef]
16.   Liu, Y.; Zou, J.; Meng, X.; Zhong, L.; Wang, Q.; Zhang, W.; Zhou, F.; Han, X. Progress in Bohai Offshore Heavy Oil Thermal Recovery. In Proceedings of the Offshore Technology Conference Asia, Kuala Lumpur, Malaysia, 22–25 March 2016.
17.   Bai, J.; Yu, F.; Jiang, Z.; Li, Y.; Shang, B.; Yan, M. First attempt of injection-production integrated technology for steam stimulation in Bohai Bay, China. In Proceedings of the International Petroleum Technology Conference, Virtual, 23 March–1 April 2021.
18.   Wei, B.; Pang, S.; Pu, W.; Lu, L.; Wang, C.; Kong, L. Mechanisms of N2 and CO2 assisted steam huff-n-puff process in enhancing heavy oil recovery: A case study using experimental and numerical simulation. In Proceedings of the SPE Middle East Oil & Gas Show and Conference, Manama, Bahrain, 6–9 March 2017.
19.   Gu, Z.; Zhang, C.; Lu, T.; Wang, H.; Li, Z.; Wang, H. Experimental analysis of the stimulation mechanism of CO_2-assisted steam flooding in ultra-heavy oil reservoirs and its significance in carbon sequestration. *Fuel* **2023**, *345*, 128188. [CrossRef]
20.   Zou, X. Investigation of Drilling Fluid System and It's Application in Yuedong Oilfield. Master's Thesis, Northeast Petroleum University, Daqing, China, 2017.
21.   Wang, Z. Geological characteristics of heavy oil reservoirs in offshore Yuedong Oilfield. *China Pet. Chem. Stand. Qual.* **2016**, *36*, 110–112.
22.   Qi, J.; Chen, F. *Structural Analysis of Cenozoic Rift Basin of Lower Liaohe-Liaodong Bay*; Geological Publishing House: Beijing, China, 1995.
23.   Lin, L. Palaeogeomorphology Characteristics of the Central up Lift Zone in Neritic Area of Liaohe and Its Control to the Sandbodies on the Both Sides. Master's Thesis, China University of Geosciences, Beijing, China, 2010.
24.   Guo, Y. Reservoir Characteristics and Prediction of Guantao Formation in Shengshun Oilfield, Liaodongdong Area. *J. Shandong Inst. Pet. Chem. Technol.* **2021**, *35*, 1753–1759.
25.   Dai, L.M.; Li, J.P.; Zhou, X.H.; Cui, Z.; Cheng, J. Depositional system of the Neogene shallow water delta in Bohai Sea area. *Lithol. Reserv.* **2007**, *19*, 75–81.
26.   Zhu, W.; Li, J.; Zhou, X.; Guo, Y. Neogene Shallow Water Deltaic System and Large Hydrocarbon Accumulations in Bohai Bay, China. *Acta Sedimentol. Sin.* **2008**, *26*, 575–582.
27.   Zhu, W. *Hydrocarbon Accumulation and Exploration in Bohai Sea*; Science Press: Beijing, China, 2009.
28.   Xu, C.; Jiang, P.; Wu, F.; Yang, P.; Li, D. Sedimentary Characteristics of the Neogene Delta in Bozhong Depression and its Significance for Oil and Gas Discovery and Exploration. *Acta Sedimentol. Sin.* **2002**, *20*, 588–593.
29.   Xu, C.; Wang, B.; Wang, F.; Wan, L.; Zhang, R. Neogene extra heavy oil accumulation model and process in Liaodong Bay depression: A case study of Lvda 5-2 N oilfield. *Acta Pet. Sin.* **2016**, *37*, 599–609.
30.   Jassam, S.A.; Al-Fatlawi, O. Development of 3D geological model and analysis of the uncertainty in a tight oil reservoir in the Halfaya Oil Field. *Iraqi Geol. J.* **2023**, *56*, 128–142. [CrossRef]
31.   Radwan, A.E. Three-dimensional gas property geological modeling and simulation. In *Sustainable Geoscience for Natural Gas Subsurface Systems*; Gulf Professional Publishing: Oxford, UK, 2022; pp. 29–49.
32.   Feng, G.; Li, Y.; Yang, Z. Performance evaluation of nitrogen-assisted steam flooding process in heavy oil reservoir via numerical simulation. *J. Pet. Sci. Eng.* **2020**, *189*, 106954. [CrossRef]
33.   Kondrat, O.; Lukin, O.; Smolovyk, L. Analysis of possibilities to increase oil recovery with the use of nitrogen in the context of deep oil deposits of the Dnipro-Donetsk oil-and-gas Ukrainian province. *Min. Miner. Depos.* **2019**, *13*, 107–113. [CrossRef]
34.   Mohamed, A.S.; Omran, A.A.; Mohamed, M.T.; Nabawy, B.S. Petrophysical analysis and hydrocarbon potential of the Matulla Formation in the Muzhil Field, central part of the Gulf of Suez, Egypt. *Min. Miner. Depos.* **2023**, *17*, 121–139. [CrossRef]
35.   Lin, J. Proceedings of the International Field Exploration and Development Conference 2023. In Proceedings of the International Field Exploration and Development Conference 2023, Wuhan, China, 20–22 September 2023.

36. Xi, C.; Qi, Z.; Zhang, Y.; Liu, T.; Shen, D.; Mu, H.; Dong, H.; Li, X.; Jiang, Y.; Wang, H. CO_2 assisted steam flooding in late steam flooding in heavy oil reservoirs. *Pet. Explor. Dev.* **2019**, *46*, 1242–1250. [CrossRef]
37. Wang, Z.; Du, H.; Li, S.; Li, S. Experimental study on gas-assisted cyclic steam stimulation under heavy-oil sandstone reservoir conditions: Effect of N_2/CO_2 ratio and foaming agent. *Geoenergy Sci. Eng.* **2023**, *228*, 211976. [CrossRef]
38. Gao, J. Study on Mechanism of CO_2-assisted Water Control for Steam Stimulation Horizontal Well with Bottom Water. Master's Thesis, China University of Petroleum, Beijing, China, 2020.
39. Cui, G.; Zhu, L.; Zhou, Q.; Ren, S.; Wang, J. Geochemical reactions and their effect on CO2 storage efficiency during the whole process of CO2 EOR and subsequent storage. *J. Greenh. Gas Control.* **2021**, *108*, 103335. [CrossRef]
40. Cui, G.; Yang, L.; Fang, J.; Qiu, Z.; Wang, Y.; Ren, S. Geochemical reactions and their influence on petrophysical properties of ultra-low permeability oil reservoirs during water and CO2 flooding. *J. Pet. Sci. Eng.* **2021**, *203*, 108672. [CrossRef]